Published in final edited form as:
Cell Rep. 2012 October 25; 2(4): 964–975. doi:10.1016/j.celrep.2012.09.002.

Pleiotrophin regulates the retention and self-renewal of hematopoietic stem cells in the bone marrow vascular niche

Heather A. Himburg[1], **Jeffrey R. Harris**[1], **Takahiro Ito**[2], **Pamela Daher**[1], **J. Lauren Russell**[1], **Mamle Quarmyne**[1], **Phuong L. Doan**[1], **Katherine Helms**[1], **Mai Nakamura**[1], **Emma Fixsen**[1], **Gonzalo Herradon**[3], **Tannishtha Reya**[2], **Nelson J. Chao**[1,4], **Sheila Harroch**[5], and **John P. Chute**[1,2]

[1]Division of Cellular Therapy, Department of Medicine, Duke University Medical Center, Durham, NC

[2]Department of Pharmacology, University of San Diego, California

[3]Pharmacology Laboratory, Department of Pharmaceutical and Food Sciences, Facultad de Farmacia, Universidad CEU San Pablo, Madrid, SP

[4]Department of Immunology, Duke University, Durham, NC

[5]Department of Neuroscience, Pasteur Institute, Paris, FR

[6]Department of Pharmacology and Cancer Biology, Duke University, Durham, NC

SUMMARY

The mechanisms through which the bone marrow (BM) microenvironment regulates hematopoietic stem cell (HSC) fate remain incompletely understood. We examined the role of the heparin-binding growth factor, pleiotrophin (PTN), in regulating HSC function in the niche. $PTN^{-/-}$ mice displayed significantly decreased BM HSC content and impaired hematopoietic regeneration following myelosuppression. Conversely, mice lacking the protein tyrosine phosphatase receptor-zeta (PTPRZ), which is inactivated by PTN, displayed significantly increased BM HSC content. Transplant studies revealed that PTN action was not HSC-autonomous but rather was mediated by the BM microenvironment. Interestingly, PTN was differentially expressed and secreted by BM sinusoidal endothelial cells within the vascular niche. Furthermore, systemic administration of anti-PTN antibody in mice substantially impaired both the homing of hematopoietic progenitor cells to the niche and the retention of BM HSCs in the niche. PTN is a secreted component of the BM vascular niche which regulates HSC self-renewal and retention in vivo.

INTRODUCTION

HSCs are capable of self-renewal and reconstitution of the entire blood and immune system in vivo. HSC fate determination in vivo is regulated by a combination of intrinsic mechanisms and environmental cues mediated via cell-cell interactions, cytokines and

Corresponding Author: John P. Chute M.D., Professor of Medicine, Professor of Pharmacology and Cancer Biology, Division of Cellular Therapy, Duke University Medical Center, Durham, NC 27710, john.chute@duke.edu, Ph 919-668-4706, Fax 919-668-1091.

secreted growth factors (Blank et al., 2008; Kiel and Morrison, 2008; Zon, 2008) While characterization of the cells within the BM microenvironment that regulate HSC fate continues to evolve (Butler et al., 2010; Calvi et al., 2003; Ding et al., 2012; Hooper et al., 2009; Kiel et al., 2005; Mendez-Ferrer et al., 2010; Salter et al., 2009; Zhang et al., 2003), the mechanisms through which BM microenvironment cells regulate HSC functions are less well understood.

We have previously shown that adult sources of endothelial cells are capable of supporting the expansion of murine and human HSCs in vitro (Chute et al., 2004; Chute et al., 2006a; Chute et al., 2005; Chute et al., 2002). Utilizing a genomic screen of primary adult human brain endothelial cells (HUBECs) which support HSC expansion in non-contact cultures (Chute et al., 2006a; Chute et al., 2005; Chute et al., 2002), we identified PTN, a heparin binding growth factor which is primarily expressed in the nervous system (Li et al., 1990), to be more than 100-fold overexpressed in HUBECs compared to non-HSC-supportive ECs (Himburg et al., 2010). We subsequently showed that in vitro treatment of murine BM HSCs with PTN, in combination with other cytokines, supported the expansion of HSCs with long-term repopulating capacity (Himburg et al., 2010). However, it remained unknown whether PTN was expressed by cells within the HSC niche which regulate HSC function in vivo or whether PTN had any physiologically relevant function in regulating HSC fate in vivo. We therefore sought to determine whether PTN was expressed by BM microenvironment cells within the HSC niche and whether modulation of PTN expression within the niche could affect the maintenance, regeneration or retention of HSCs in vivo. Here, we show that PTN is uniquely expressed and secreted by BM sinusoidal ECs within the HSC vascular niche and has an important role in regulating HSC self-renewal and retention in the BM.

RESULTS

PTN Regulates HSC Self-Renewal and Is Necessary for Hematopoietic Regeneration In Vivo

We first examined the hematologic phenotype of mice bearing a constitutive deletion of PTN (PTN $^{-/-}$ mice) versus littermate control PTN $^{+/+}$ mice. Knockout of PTN in the mouse strain was confirmed by real time PCR analysis (Figure 1A). Eight week old PTN $^{-/-}$ mice displayed no significant differences in peripheral blood (PB) complete blood counts or spleen size (Figure S1). We also observed no differences in BM vascular density between PTN $^{-/-}$ mice and PTN $^{+/+}$ mice (data not shown). However, adult PTN $^{-/-}$ mice contained significantly decreased BM c-kit^{+}sca-1^{+}lineage^{-} (KSL) stem/progenitor cells as well as BM colony forming unit-spleen day 12 cells (CFU-S12)(Figure 1B). Furthermore, PTN $^{-/-}$ mice contained significantly decreased numbers of BM SLAM-receptor (CD150^{+}CD48^{-} CD41^{-}) – positive KSL (SLAM^{+}KSL) cells (Kiel et al., 2005) compared to PTN$^{+/+}$ mice, reflecting a deficit in phenotypic HSCs (Figure 1B). Importantly, competitive transplantation assays of BM 34^{-}KSL cells, which are highly enriched for HSCs (Himburg et al., 2010), into lethally irradiated congenic mice confirmed a marked decrease in long-term (LT)-HSC content in PTN $^{-/-}$ mice compared to PTN $^{+/+}$ mice. At 12 weeks following competitive transplantation, donor CD45.2^{+} PB cell engraftment was 7-fold lower in mice that were transplanted with BM 34^{-}KSL cells from PTN $^{-/-}$ mice compared to recipients of BM 34^{-}KSL cells from PTN $^{+/+}$ mice (mean 5% vs. 35%, Figure 1C). Multilineage engraftment of myeloid cells, erythroid cells, B cells and T cells was also significantly lower in mice transplanted with BM HSCs from PTN $^{-/-}$ mice compared to recipients transplanted with BM HSCs from PTN $^{+/+}$ mice (Figure 1D). Analysis over time revealed that mice transplanted with BM HSCs from PTN $^{-/-}$ mice had 5-20 fold decreased donor cell repopulation between 4 weeks and 20 weeks post-transplant compared to mice transplanted with HSCs from PTN $^{+/+}$ mice, confirming a loss of both short-term (ST)- and LT-HSCs in PTN $^{-/-}$ mice (Figure 1C). Poisson statistical analysis of a limiting dilution transplant assay

demonstrated that the competitive repopulating unit (CRU) frequency within PTN $^{-/-}$ mice was 11-fold decreased (1 in 66 cells, Confidence Interval (CI): 1/37 - 1/119) compared to the CRU frequency in PTN $^{+/+}$ mice (1 in 6, CI: 1/2 - 1/14, Figure 1E). Taken together, these results demonstrate that PTN regulates the maintenance of the BM HSC pool.

Since deletion of PTN caused a substantial reduction in BM HSC content in vivo, we next sought to determine if PTN deletion affected hematopoietic regeneration following myelosuppressive injury. We irradiated adult PTN $^{-/-}$ mice and PTN $^{+/+}$ mice with 700 cGy, a myelosuppressive radiation dose, and compared their survival through day +30. Sixty-nine percent (11 of 16) of the PTN $^{+/+}$ mice remained alive and well through day +30 (Figure 1F). In contrast, none of the PTN $^{-/-}$ mice (0 of 7) survived past day +18 post-TBI, indicating markedly increased radiosensitivity in PTN $^{-/-}$ mice. Commensurate with this, PTN $^{-/-}$ mice displayed severely decreased BM progenitor cell content at day +20, whereas PTN $^{+/+}$ mice showed evidence of recovery of the BM progenitor cell compartment (Figure 1G). Taken together, these results demonstrate that PTN is essential for hematopoietic regeneration and survival following radiation-induced myelosuppression.

PTN Regulates the HSC Pool in a Microenvironment-Dependent Manner

In order to determine whether PTN signaling was HSC-autonomous or dependent on the BM microenvironment, we transplanted BM cells from CD45.1^{+} Bl6.SJL mice into lethally irradiated PTN $^{-/-}$ mice or PTN $^{+/+}$ mice (CD45.2^{+}) and compared the hematopoietic phenotypes of these chimeric mice. At 8 weeks post-transplant, recipient mice demonstrated > 95% donor chimerism (mean 96.4% donor cells in WT;PTN $^{+/+}$ mice and 95.2% in WT;PTN $^{-/-}$ mice, n = 8-9 mice/group). Adult PTN $^{-/-}$ mice that were transplanted with BM cells from Bl6.SJL mice (WT;PTN $^{-/-}$ mice) displayed significantly decreased numbers of BM KSL cells, CFU-S12 and SLAM^{+}KSL HSCs compared to age matched WT;PTN $^{+/+}$ mice (Figure 1H). Importantly, mice that were competitively transplanted with BM from WT;PTN $^{-/-}$ mice also displayed significantly decreased multilineage donor cell repopulation between 4 weeks and 30 weeks post-transplant compared to mice transplanted with the identical dose of BM cells from WT;PTN $^{+/+}$ mice (Figure 1I). Secondary transplantation of BM cells from the primary transplant recipients demonstrated that secondary mice in the WT;PTN $^{-/-}$ group had 4-fold decreased donor cell engraftment at 8 weeks post-transplant compared to secondary recipients in the WT;PTN $^{+/+}$ group (mean donor CD45.1^{+} cells: 0.5% ± 0.2 vs. 2.0% ± 0.7, p = 0.04, n=8-9/group). These results demonstrate that PTN production by the BM microenvironment is necessary regeneration of the HSC pool following BM transplantation.

Since PTN was necessary for normal HSC reconstitution in vivo following BM transplantation, we next tested whether pharmacologic administration of PTN could accelerate HSC reconstitution in a clinically relevant model of HSC transplantation. We transplanted limiting doses (0.5 - 1 × 10^{6} cells) of human CB mononuclear cells intravenously into NOD/SCID IL2R-$\gamma^{-/-}$ (NSG) mice and compared human hematopoietic reconstitution over time in mice which were treated intraperitoneally with 2 – 4 μg PTN or saline on days +7, +10 and +13 post-transplant. Peripheral blood was analyzed at 4 and 8 weeks post-transplant for human CD45^{+} cell engraftment. PTN-treated mice demonstrated significantly increased human CD45^{+} cell repopulation compared to saline-treated mice over time (4 weeks: mean 10.9% huCD45^{+} vs. 1.4%; 8 weeks: mean 9.9% vs. 1.9%, n=11-14 mice/group, Figure 1J). Importantly, NSG mice that were treated with PTN also contained > 10-fold increased human hematopoietic progenitor cell content in the BM at 8 weeks post-transplant compared to saline-treated controls (Figure 1J). These results show that PTN promotes human hematopoietic stem/progenitor cell regeneration in vivo following transplantation and illustrate the translational potential of PTN administration as a means to accelerate human hematopoietic reconstitution, particularly in settings wherein the HSC

dose is limiting, such as human CB transplantation (Laughlin et al., 2004; Rocha et al., 2004).

Deletion of PTPRZ Expands the HSC Pool In Vivo

In the nervous system, PTN can mediate proliferative signals via binding and inhibition of the transmembrane receptor, PTPRZ (Meng et al., 2000; Raulo et al., 1994; Stoica et al., 2001). We sought to determine whether PTN mediates HSC self-renewal via inactivation of PTPRZ signaling in HSCs. To achieve this, we examined the hematopoietic phenotype of Ptprz1$^{-/-}$ mice compared to Ptprz1$^{+/+}$ mice. Real time PCR confirmed the deletion of the full length mRNA transcript for PTPRZ in the mutant mice (Figure 2A). Interestingly, 8 week old Ptprz1$^{-/-}$ mice demonstrated significantly increased WBCs, hemoglobin and platelet counts compared to age matched Ptprz1$^{+/+}$ mice (Figure 2B). Ptprz1$^{-/-}$ mice also displayed significantly increased total BM cells, KSL progenitor cells, CFU-S12 and SLAM^{+}KSL HSCs compared to Ptprz1$^{+/+}$ mice (Figure 2C,D). Competitive repopulating assays demonstrated that mice transplanted with BM 34^{-}KSL cells from Ptprz1$^{-/-}$ mice had 6-fold increased donor CD45.2^{+} cell engraftment at 12 weeks post-transplant compared to mice transplanted with BM cells from Ptprz1$^{+/+}$ mice (Figure 2E). Mice transplanted with HSCs from Ptprz1$^{-/-}$ mice also displayed normal and increased multilineage donor myeloid, erythroid, T cell and B cell repopulation compared to recipients of BM from Ptprz1$^{+/+}$ mice, confirming that deletion of PTPRZ did not alter the normal differentiation capacity of BM HSCs (Figure 2F). Mice transplanted with BM cells from Ptprz1$^{-/-}$ mice also demonstrated 5-fold and 10-fold increased donor CD45.2^{+} cell engraftment at 4 weeks and 16 weeks post-transplant compared to mice transplanted with BM cells from Ptprz1$^{+/+}$ mice, confirming that deletion of PTPRZ increased both ST- and LT-HSC content in vivo (Figure 2E). Poisson statistical analysis of donor cell engraftment at 12 weeks from a limiting dilution assay demonstrated a CRU frequency of 1 in 23 in Ptprz1$^{-/-}$ mice (CI: 1/13 to 1/42) compared to 1 in 72 in Ptprz1$^{+/+}$ mice (CI:1/27 to 1/189, Figure 2G). Therefore, deletion of PTPRZ was sufficient to expand the BM HSC pool in vivo and implicated PTPRZ as the receptor which mediates PTN signaling in HSCs. As further evidence that PTPRZ is necessary for PTN-mediated expansion of HSCs, we found that PTN treatment of BM KSL cells from PTPRZ$^{+/+}$ mice caused a significant expansion of KSL cells in vitro, whereas PTN treatment of BM KSL cells from PTPRZ $^{-/-}$ mice failed to expand KSL cells in culture (Figure S2). Of note, we have followed Ptprz1$^{-/-}$ mice through 12 months of age and these mice display no evidence of splenomegaly, lymphadenopathy, leukemia or decreased survival compared to Ptprz1$^{+/+}$ mice; these data suggest that deletion of PTPRZ alone does not confer clonal myeloproliferative or lymphoproliferative disease in mice (Figure S3).

PTPRZ Signaling is HSC-Autonomous

In order to determine if PTN signaling through PTPRZ was HSC-autonomous or mediated via indirect effects on other BM cell types, we transplanted lethally irradiated Bl6.SJL mice (CD45.1^{+}) with BM cells from Ptprz1$^{-/-}$ or Ptprz1$^{+/+}$ mice (CD45.2^{+}) to create Ptprz1$^{-/-}$;WT mice and Ptprz1$^{+/+}$;WT mice. At 8 weeks post-transplant, recipient mice were ≥ 95% CD45.2^{+}, confirming full donor chimerism (Figure 2H). At this time point, we examined the BM stem/progenitor cell content in both groups of mice. Ptprz1$^{-/-}$;WT mice demonstrated significant increases in BM KSL cells, CFU-S12 and SLAM^{+}KSL HSCs compared to Ptprz1$^{+/+}$;WT mice (Figure 2I). These results demonstrated that PTPRZ-mediated regulation of the HSC pool was HSC-autonomous and independent of PTPRZ signaling in the BM microenvironment.

BM ECs and CXCL12^{+} Reticular Cells Express PTN in the HSC Niche

Our transplant studies suggest that maintenance of the HSC pool is dependent upon production of PTN by the BM microenvironment. We next sought to determine which cells

within the BM microenvironment produce PTN. Immunostaining of adult mice femurs from PTN-GFP mice revealed that a subset of VE-cadherin$^+$ BM ECs co-expressed PTN, as did VEGFR3$^+$ sinusoidal ECs (Figure 3A,B) (Butler et al., 2010; Hooper et al., 2009; Salter et al., 2009). Similarly, a subset of CXCL12 (SDF-1)$^+$ cells, which appeared to be perivascular, also co-expressed PTN, whereas the majority of osterix$^+$ osteoblasts did not express PTN (Figure 3C-E)(Tang et al., 2011). Taken together, these results demonstrated a differential expression of PTN by BM ECs and perhaps by CXCL12-abundant reticular cells (CARs)(Sugiyama et al., 2006). We further determined by ELISA that PTN was concentrated within the BM serum of C57Bl6 mice but was not detectable in PB serum (Figure S4); in addition, PTN was highly enriched in the conditioned media from primary BM ECs from C57Bl6 mice, confirming that BM ECs secrete PTN (Figure S4). These results show that PTN is differentially expressed and secreted by principal components of the BM vascular niche and is a paracrine factor for BM stem/progenitor cells in vivo.

In order to further characterize the cells within the BM niche that expressed PTN, we performed FACS analysis on BM CD45$^-$PTN$^+$ cells and analyzed for surface expression of the EC marker, VE-cadherin. FACS analysis revealed a distinct population of VE-cadherin$^+$PTN$^+$ cells in the BM (Figure 3F). We then performed gene expression analysis of FACS-sorted VE-cadherin$^+$PTN$^+$ cells, which revealed enrichment for VEGFR2 and VEGFR3, which are markers of BM sinusoidal endothelium (Hooper et al., 2009)(Table 1). Interestingly, VE-cadherin$^+$PTN$^+$ cells were also enriched for expression of CXCL12 and the leptin receptor (lepR), proteins which have been shown to be expressed by both perivascular stromal cells and sinusoidal ECs (Dar et al., 2005; Ding et al., 2012; Ikejima et al., 2004; Sugiyama et al., 2006). VEcadherin$^+$PTN$^+$ cells lacked expression of Nestin, a marker of BM mesenchymal stromal cells (MSCs) (Mendez-Ferrer et al., 2010).

Lastly, to determine the anatomic relationship between PTN$^+$ cells and HSCs in the BM, we immunostained femurs from PTN-GFP mice to detect CD150$^+$CD48$^-$CD41$^-$lineage$^-$ cells. As previously described, we found CD150$^+$CD48$^-$CD41$^-$lineage$^-$ cells to be rare in the BM (Kiel et al., 2005; Mendez-Ferrer et al., 2010). However, the majority (82.3%, 51 of 62) of the CD150$^+$CD48$^-$CD41$^-$lineage$^-$ cells were found to be in contact with or closely adjacent to PTN$^+$ cells (30 images, 5 femur sections; Figure 3G). Taken together with our functional studies of PTN$^{-/-}$ mice, these results suggest an anatomic and functional relationship between BM HSCs and PTN$^+$ cells in the vascular niche.

PTN regulates hematopoietic progenitor cell (HPC) homing to the BM niche

Since we have shown here that PTN is expressed by sinusoidal BM ECs within the vascular niche, we sought to determine whether PTN$^+$ ECs regulate hematopoietic stem/progenitor cell (HSPC) homing to the niche. Adult C57Bl6 mice were injected intravenously with either 50 μg of a specific, neutralizing anti-PTN antibody (R&D Systems) or 50 μg IgG and, after 30 minutes, were infused with 2×10^5 BM Sca-1$^+$lin$^-$ progenitor cells from Ubiquitin C-GFP (UBC-GFP) mice. At 18 hours post-transplant, mice were sacrificed and BM cells were analyzed by FACS to compare the homing of GFP$^+$ cells to the BM in each group. Mice that were pre-treated with anti-PTN antibody displayed a significant decrease in donor HSPC homing to the BM compared to IgG-treated recipient mice (Figure 4A,B). These results suggested that PTN is required for the proper homing of HSPCs to the BM following transplantation. In order to determine the specific effect that anti-PTN administration had on the homing of transplanted HPCs, we performed intravital imaging using confocal microscopy to observe intravenously transplanted BM lin$^-$GFP$^+$ cells homing within the calvarial BM endothelium in dsRed mice, as previously described (Lo Celso et al., 2011). Mice that were pre-treated with IgG and then intravenously transplanted with 3×10^6 BM lin$^-$GFP$^+$ cells demonstrated dynamic transmigration of GFP$^+$ cells from the BM vascular space into the BM parenchymal space between 1 to 4 hours post-transplant (Figure 4C,D

and Movies S1 and S2). In contrast, mice that were pre-treated with anti-PTN and then transplanted with equal doses of BM $lin^{-}GFP^{+}$ cells demonstrated a substantial defect in lodgment along BM endothelium and in transmigration across the BM vasculature into the HSC niche (Figure 4C,D **and** Movies S1 and S2). Coupled with the demonstration that anti-PTN quantitatively decreased HSPC homing to the niche, these data suggested an essential role for PTN in regulating the lodgment and/or transmigration of HSPCs from the BM vasculature into the HSC niche. Of note, to confirm that systemically administered anti-PTN mediated effects directly upon the BM vascular endothelium, we also show that mice injected with 50 μg anti-PTN-DyLight650 antibody displayed specific binding of the antibody to the intimal endothelial layer of the BM vasculature, whereas mice injected with 50 μg IgG-DyLight650 showed no binding to BM ECs (Figure 4E).

HSPC homing to the BM niche is regulated by numerous cooperative mechanisms including HSPC rolling, lodgment and transmigration through BM sinusoidal vasculature, mediated by VLA4-VCAM and CD44-Hyaluronic Acid interactions between HSPCs and BM ECs and via the CXCR4-CXCL12 axis (Avigdor et al., 2004; Kahn et al., 2004; Papayannopoulou et al., 1995). We performed in vitro migration assays in which 2×10^5 BM $ckit^{+}lin^{-}$ cells were placed in the upper chamber of transwell cultures, with either 200 ng PTN, 200 ng SDF-1 (CXCL12) or media in the lower chamber. At 4 hours of culture, we observed no migration of HSPCs toward PTN, whereas 35% of HSPCs migrated toward SDF1 (Figure 4F). These data suggested that PTN alone did not provide a gradient for HSPC migration. When HSPCs were pre-incubated for 1 hour with PTN, we observed a significant increase in HSPC migration toward SDF1, suggesting that PTN augments HSPC migration toward an SDF1 gradient (Figure 4F). However, incubation with PTN did not upregulate CXCR4 or VLA4 expression on BM $ckit^{+}lin^{-}$ cells, suggesting that PTN regulates HSPC homing through an alternative mechanism (Figure 4F).

Administration of anti-PTN promotes HSPC mobilization

Our results suggest that PTN has an important role in regulating HSPC homing to the BM niche. We hypothesized further that PTN might also regulate HSC retention in the niche and that systemic administration of anti-PTN might promote HSPC mobilization. To test this hypothesis, adult C57Bl6 mice were treated with either 50 μg IgG, 50 μg anti-PTN, or the CXCR4 antagonist, AMD3100 (50 μg) or AMD3100 + anti-PTN. At 1 hour post-treatment, peripheral blood was collected and analyzed for mobilization of $ckit^{+}sca\text{-}1^{+}lin^{-}$ cells (KSL cells), which are enriched for HSPCs. Interestingly, treatment with anti-PTN alone significantly increased the number of KSL cells in the PB at 1 hour post-treatment compared to IgG-treated control mice (Figure 4G,H). As expected, AMD3100, which is utilized clinically to mobilize HSPCs (Malard et al., 2012), also promoted HSPC mobilization. Importantly, the combination of AMD3100 and anti-PTN caused a 2-fold increase the mobilization of BM KSL cells compared to the effect of AMD3100 treatment alone (Figure 4G,H). Taken together, these data suggest that PTN also regulates the retention of HSPCs in the BM niche and cooperates with the CXCR4-SDF1 axis in this regard.

DISCUSSION

Recent studies have implicated several different cell types within the BM microenvironment has having an important roles in regulating HSC self-renewal and retention in vivo (Butler et al., 2010; Calvi et al., 2003; Ding et al., 2012; Hooper et al., 2009; Kiel et al., 2005; Mendez-Ferrer et al., 2010; Salter et al., 2009; Zhang et al., 2003). However, the mechanisms through which BM microenvironment cells regulate HSC functions in vivo remain incompletely understood. Here, we show that PTN, a heparin binding growth factor, is expressed by sinusoidal ECs within the BM vascular niche and regulates the maintenance

of the HSC pool in vivo. Furthermore, genetic deletion of PTPRZ, a receptor for PTN which is expressed by HSCs, caused a significant expansion of the HSC pool in vivo. This observed effect is consistent with the established function of PTN as inactivating PTPZ phosphatase activity upon receptor binding. The observed deficit in HSC numbers coupled with only slight reductions in PB complete blood counts in PTN $^{-/-}$ mice suggests the possibility of compensation by other factors (Herradon et al., 2005) in PTN $^{-/-}$ mice. However, PTN appears to be indispensable for hematopoietic regeneration to occur following myelosuppression since PTN $^{-/-}$ mice had significantly increased mortality following a myelosuppressive dose of TBI (700 cGy), coupled with a severe deficit in the recovery of BM progenitor cells compared to PTN $^{+/+}$ mice. These results reveal an essential role for PTN in regulating hematopoietic regeneration following injury.

Recently, cellular components of a BM vascular niche for HSCs have been identified, including VEGFR2^{+}VEGFR3^{+} sinusoidal ECs, CXCL12-abundant reticular cells (CARs) and lepR^{+} perivascular cells, which are essential for the maintenance of the HSC pool during homeostasis (Ding et al., 2012; Hooper et al., 2009; Sugiyama et al., 2006). Nestin^{+} MSCs have also been shown to contribute to both the vascular and endosteal niches for HSCs in vivo (Mendez-Ferrer et al., 2010). However, the signaling mechanisms through which cells within the BM vascular niche regulate HSC homeostasis or regeneration are not well understood. Here, we demonstrate via immunohistochemical and FACS analysis that PTN is expressed uniquely by VE-cadherin^{+} ECs that co-express VEGFR2 and VEGFR3^{+}, consistent with BM sinusoidal ECs (Hooper et al., 2009). Interestingly, PTN^{+} ECs also express CXCL12 and lepR, which can be expressed by both sinusoidal ECs and perivascular reticular cells (Dar et al., 2005; Ding et al., 2012; Ikejima et al., 2004; Sugiyama et al., 2006). Of note, a prior study suggested that calvarial bone osteoblasts expressed PTN (Tezuka et al., 1990), but we found little evidence that osterix^{+} bone lineage cells expressed PTN in the BM. Commensurate with our findings that PTN was highly expressed by BM sinusoidal ECs, PTN was highly concentrated in BM supernatants and in the conditioned media of primary BM sinusoidal ECs in culture, but was undetectable in the PB of wild type mice. These results, coupled with the observed deficit in HSC repopulating cell content in WT;PTN$^{-/-}$ mice, suggest that PTN is an important paracrine factor for HSCs within the vascular niche.

In addition to their role in regulating the maintenance of the HSC pool in vivo, BM sinusoidal ECs regulate the rolling, lodgment and transmigration of transplanted hematopoietic stem/progenitor cells from the vascular space into HSC niches (Avigdor et al., 2004; Papayannopoulou et al., 1995). For example, VLA4-VCAM1 and CD44-Hyaluronic acid interactions between HSPCs and BM ECs control the initial steps in the homing of HSPCs across the vascular endothelium (Avigdor et al., 2004; Papayannopoulou et al., 1995). Since PTN is strongly expressed by BM sinusoidal ECs, we sought to determine whether PTN also regulated HSPC migration and homing to the niche. Interestingly, administration of a single dose of anti-PTN antibody substantially inhibited HSPC homing to the niche. Furthermore, intravital imaging revealed that transplanted HSPCs displayed impaired lodgment along the BM endothelium and deficient transmigration from the vascular space into the HSC niche. These data suggest that HSPC anchoring to PTN on sinusoidal ECs may be a critical step in HSPC homing to the BM. In vitro migration assays revealed that HSPCs did not migrate toward a PTN gradient but pre-treatment with PTN did augment HSPC migration toward SDF1. Since PTN treatment did not upregulate CXCR4 or VLA4 expression on HSPCs, PTN may facilitate HSPC homing toward SDF1 via a mechanism yet to be identified.

In addition to its evident role in regulating the homing of HSPCs to the BM, PTN also regulates the retention of HSPCs in the niche. Administration of a single dose of anti-PTN

caused a 2-fold increase in PB HSPCs at 1 hour post-exposure compared to isotype-treated mice and a similar increase in HSPC mobilization was observed when anti-PTN was combined with AMD3100, a CXCR4 antagonist which is used in clinical practice to mobilize human HSPCs. The rapidity of the effect of anti-PTN administration on HSPC mobilization suggests that PTN plays an important role in the retention of HSPCs in the niche. Moreover, the doubling of HSPC mobilization when anti-PTN was combined with AMD3100 suggests an additive or synergistic role for PTN in modulating HSPC retention via the CXCR4-SDF1 axis. These results also suggest an important potential clinical application for anti-PTN for the mobilization of HSPCs in patients undergoing stem cell transplantation.

Istvanffy et al. recently reported that deletion of PTN in the BM microenvironment was associated with a gain of long-term HSC function compared to mice which retained PTN in the marrow (Istvanffy et al., 2011). Important differences between the mouse models utilized may explain the apparently divergent results between this study and ours: first, we utilized PTN $^{-/-}$ mice (C57Bl6 background, Jackson Laboratory) and syngeneic (B6.SJL) recipient mice for CRU transplantation studies and for the generation of WT;PTN$^{-/-}$ mice to assess effects of PTN on HSC content. Since these donor and recipient mice were genetically identical, there were no immunological factors which could confound estimates of HSC content. Conversely, in the study by Istvanffy et al., the competitive repopulation assays involved allogeneic transplantation of BM from PTN $^{-/-}$ mice (129.B6 strain) into mixed strain (129S2 × Ly5.1) recipient mice and chimeric WT;PTN$^{-/-}$ mice were generated by transplantation of BM cells from B6.SJL mice into 129.B6 mice. Therefore, immunologic processes such as graft rejection and graft versus host reaction, or the effects of PTN on these immune processes, could have significantly affected estimates of HSC content in this allogeneic model independent of any direct effects of PTN on the HSC pool. Second, we have demonstrated full deletion of PTN in BM cells from PTN $^{-/-}$ mice, whereas deletion of PTN in vivo was not reported in the prior study (Istvanffy et al., 2011). Lastly, in this study we utilized purified HSCs (CD34^{-}KSL cells) for competitive transplantation assays to allow precise determination of effects of PTN deletion on HSC content and function, whereas in the prior study, whole BM cells were utilized, allowing for the possibility of effects on adventitious cells in the graft to affect HSC estimates.

Much remains unknown regarding the mechanisms through which BM microenvironment cells regulate HSC functions in vivo. Here, we provide the first evidence that BM sinusoidal ECs uniquely express a secreted protein, PTN, which regulates the maintenance, regeneration and retention of HSCs in the vascular niche. PTN represents a unique target for pharmacologic approaches to modulate HSC function in vivo.

EXPERIMENTAL PROCEDURES

Mice

All animal procedures were performed in accordance with a Duke University IACUC-approved animal use protocol. Embryos from mice bearing a constitutive deletion of PTN (Ochiai et al., 2004) were obtained from the RIKEN Institute (Tsukuba, Japan) by the Jackson Laboratory (Bar Harbor, ME) and re-derived in a C57BL6 background. Mice bearing a constitutive deletion of the PTN receptor, PTPRZ were a generous gift from Dr. Sheila Harroch of L'Institut Pasteur, Paris, FR (Harroch et al., 2002; Harroch et al., 2000). Sperm from PTN-GFP mice developed as part of the GENSAT Project Rockefeller University was obtained from the MMRRC and the strain was re-derived in a C57BL6 background.

Isolation of Murine BM HSCs

BM HSCs were collected from all mice as previously described (Himburg et al., 2010). Briefly, collected BM was first treated with RBC-lysis buffer (Sigma Aldrich) and lineage committed cells were removed using a lineage depletion column (Miltenyi Biotec Inc, Auburn CA). Lin^- cells were stained with FITC-conjugated anti-CD34 (eBioscience, San Diego, CA), PE-conjugated anti-sca-1, and APC-conjugated anti-ckit (Becton Dickinson [BD], San Jose, CA), or isotype controls. Sterile cell sorting was conducted on a BD FACS-Aria cytometer. Purified $CD34^-c\text{-}kit^+sca\text{-}1^+lin^-$ (34^-KSL) subsets were collected into Iscove's Modified Dulbecco's Medium (IMDM) + 10% FBS + 1% pcn/strp.

Colony Forming Cell (CFC) and CFU-S12 Assay

CFC assays [colony-forming unit-granulocyte monocyte (CFU-GM), burst-forming unit-erythroid (BFU-E), and colony-forming unit-mix (CFU-GEMM)] were performed in triplicate as we have previously described (Chute et al., 2005; Chute et al., 2002). Briefly, 5,000 cells from each condition were placed in MethoCult (StemCell Technologies, Vancouver, Canada) for 14 days, and total colonies were calculated. BM HSC content in the mutant mice was assayed by colony forming unit spleen day 12 assay (CFU-S12). RBC-depleted BM was transplanted at a dose of 1×10^5 cells/mouse into lethally irradiated (950 cGy) C57Bl6 mice. At day 12 post-transplant, mice were euthanized and the spleens were collected. The numbers of hematopoietic colonies on each spleen were counted.

Competitive Repopulating Unit (CRU) Assay

BM 34^-KSL cells from the $PTN^{-/-}$, $Ptprz1^{-/-}$ mice and $PTN^{+/+}$ and $Ptprz1^{+/+}$ mice, carrying the CD45.2 allele, were isolated by FACS (Himburg et al., 2010). Recipient B6.SJL animals, expressing the CD45.1 allele, received 950 cGy total body irradiation (TBI) using a Cs137 irradiator and then transplanted via tail vein injection with 5, 10, 30 or 100 BM 34^-KSL cells. Non-irradiated host BM MNCs (1×10^5 cells/mouse) were injected as competitor cells. Multi-lineage hematologic reconstitution was monitored in the peripheral blood (PB) by flow cytometry, as previously described (Chute et al., 2007; Himburg et al., 2010), at 4, 8, 12, 16 and 20 weeks post-transplant. PB was collected via submandibular puncture and stained with anti-lineage marker antibodies as previously described (Himburg et al., 2010). Animals were considered to be engrafted if donor CD45.2 cells were present at ≥1%. Competitive Repopulating Unit (CRU) calculations were performed using L-Calc software (Stem Cell Technologies) (Chute et al., 2005; Chute et al., 2006b).

PTN Reporter Mice

PTN-GFP reporter mice (Jackson Laboratory) were given intravenous injection of 200 ug of rat anti-mouse Alexa Fluor 647 VE-cadherin antibody in PBS. The mice were sacrificed within one hour of injection and the bone marrow was flushed through a 30 um filter in Hanks' balanced salt solution with Ca^{++} and Mg^{++}. The portion of the bone marrow retained in the 30 um filter was collected and mechanically disrupted by pipetting. The filter-retained cells were then stained with PerCP conjugated CD45 and FACs sorted to obtain the $CD45^-VEcadherin^+PTN^+$ and $CD45^-VEcadherin^-PTN^+$ cells. These populations were compared to the $CD45^+PTN^-$ cell population for RT-PCR analysis.

PTN Treatment of $Ptprz1^{-/-}$ Cells In Vitro

$CD34^-KSL$ cells were isolated from $Ptprz1^{-/-}$ and $Ptprz^{+/+}$ mice and cultured for 7 days in IMDM containing 10%FBS, 1% pen-strep, 125 ng/ml stem cell factor, 50 ng/ml Flt-3 ligand, and 20 ng/ml thrombopoietin either with or without 100 ng/ml PTN. Following culture, the progeny were analyzed for total KSL cell expansion.

Human Cord Blood Transplant Model

Human cord blood (CB) units were purified for mononuclear cells (MNCs) using a density gradient separation in Ficoll-HyPaque followed by red blood cell lysis. 0.5 - 1×10^6 human CB MNCs were transplanted into 6 week old NOD/SCID IL2R-gamma null (NSG) mice conditioned with 250 cGy radiation on a Cesium source. Following transplantation the mice were treated i.p. on days +7, +10, and +13 post-transplant with 2 - 4 μg PTN or saline. Peripheral blood was drawn retroorbitally at 4 and 8 weeks post-transplant to assess human $CD45^+$ cell engraftment.

Supplementary Material

Refer to Web version on PubMed Central for supplementary material.

Acknowledgments

The authors wish to thank Dr. Joel Ross for assistance with graphical art. This work was supported, in part, by National Institute for Allergy and Infectious Diseases grant AI067798-06 (JPC) and National Heart, Lung and Blood Institute grant HL086998-01 (JPC).

REFERENCES

Avigdor A, Goichberg P, Shivtiel S, Dar A, Peled A, Samira S, Kollet O, Hershkoviz R, Alon R, Hardan I, et al. CD44 and hyaluronic acid cooperate with SDF-1 in the trafficking of human CD34+ stem/progenitor cells to bone marrow. Blood. 2004; 103:2981–2989. [PubMed: 15070674]

Blank U, Karlsson G, Karlsson S. Signaling pathways governing stem-cell fate. Blood. 2008; 111:492–503. [PubMed: 17914027]

Butler JM, Nolan DJ, Vertes EL, Varnum-Finney B, Kobayashi H, Hooper AT, Seandel M, Shido K, White IA, Kobayashi M, et al. Endothelial cells are essential for the self-renewal and repopulation of Notch-dependent hematopoietic stem cells. Cell stem cell. 2010; 6:251–264. [PubMed: 20207228]

Calvi LM, Adams GB, Weibrecht KW, Weber JM, Olson DP, Knight MC, Martin RP, Schipani E, Divieti P, Bringhurst FR, et al. Osteoblastic cells regulate the haematopoietic stem cell niche. Nature. 2003; 425:841–846. [PubMed: 14574413]

Chute JP, Muramoto G, Fung J, Oxford C. Quantitative analysis demonstrates expansion of SCID-repopulating cells and increased engraftment capacity in human cord blood following ex vivo culture with human brain endothelial cells. Stem Cells. 2004; 22:202–215. [PubMed: 14990859]

Chute JP, Muramoto GG, Dressman HK, Wolfe G, Chao NJ, Lin S. Molecular profile and partial functional analysis of novel endothelial cell-derived growth factors that regulate hematopoiesis. Stem Cells. 2006a; 24:1315–1327. [PubMed: 16373696]

Chute JP, Muramoto GG, Fung J, Oxford C. Soluble factors elaborated by human brain endothelial cells induce the concomitant expansion of purified human BM CD34+CD38- cells and SCID-repopulating cells. Blood. 2005; 105:576–583. [PubMed: 15345596]

Chute JP, Muramoto GG, Salter AB, Meadows SK, Rickman DW, Chen B, Himburg HA, Chao NJ. Transplantation of vascular endothelial cells mediates the hematopoietic recovery and survival of lethally irradiated mice. Blood. 2007; 109:2365–2372. [PubMed: 17095624]

Chute JP, Muramoto GG, Whitesides J, Colvin M, Safi R, Chao NJ, McDonnell DP. Inhibition of aldehyde dehydrogenase and retinoid signaling induces the expansion of human hematopoietic stem cells. Proc Natl Acad Sci U S A. 2006b; 103:11707–11712. [PubMed: 16857736]

Chute JP, Saini AA, Chute DJ, Wells MR, Clark WB, Harlan DM, Park J, Stull MK, Civin C, Davis TA. Ex vivo culture with human brain endothelial cells increases the SCID-repopulating capacity of adult human bone marrow. Blood. 2002; 100:4433–4439. [PubMed: 12393435]

Dar A, Goichberg P, Shinder V, Kalinkovich A, Kollet O, Netzer N, Margalit R, Zsak M, Nagler A, Hardan I, et al. Chemokine receptor CXCR4-dependent internalization and resecretion of

functional chemokine SDF-1 by bone marrow endothelial and stromal cells. Nat Immunol. 2005; 6:1038–1046. [PubMed: 16170318]

Ding L, Saunders TL, Enikolopov G, Morrison SJ. Endothelial and perivascular cells maintain haematopoietic stem cells. Nature. 2012; 481:457–462. [PubMed: 22281595]

Harroch S, Furtado GC, Brueck W, Rosenbluth J, Lafaille J, Chao M, Buxbaum JD, Schlessinger J. A critical role for the protein tyrosine phosphatase receptor type Z in functional recovery from demyelinating lesions. Nat Genet. 2002; 32:411–414. [PubMed: 12355066]

Harroch S, Palmeri M, Rosenbluth J, Custer A, Okigaki M, Shrager P, Blum M, Buxbaum JD, Schlessinger J. No obvious abnormality in mice deficient in receptor protein tyrosine phosphatase beta. Mol Cell Biol. 2000; 20:7706–7715. [PubMed: 11003666]

Herradon G, Ezquerra L, Nguyen T, Silos-Santiago I, Deuel TF. Midkine regulates pleiotrophin organ-specific gene expression: evidence for transcriptional regulation and functional redundancy within the pleiotrophin/midkine developmental gene family. Biochem Biophys Res Commun. 2005; 333:714–721. [PubMed: 15985215]

Himburg HA, Muramoto GG, Daher P, Meadows SK, Russell JL, Doan P, Chi JT, Salter AB, Lento WE, Reya T, et al. Pleiotrophin regulates the expansion and regeneration of hematopoietic stem cells. Nat Med. 2010; 16:475–482. [PubMed: 20305662]

Hooper AT, Butler JM, Nolan DJ, Kranz A, Iida K, Kobayashi M, Kopp HG, Shido K, Petit I, Yanger K, et al. Engraftment and reconstitution of hematopoiesis is dependent on VEGFR2-mediated regeneration of sinusoidal endothelial cells. Cell Stem Cell. 2009; 4:263–274. [PubMed: 19265665]

Ikejima K, Lang T, Zhang YJ, Yamashina S, Honda H, Yoshikawa M, Hirose M, Enomoto N, Kitamura T, Takei Y, et al. Expression of leptin receptors in hepatic sinusoidal cells. Comp Hepatol. 2004; 3(Suppl 1):S12. [PubMed: 14960164]

Istvanffy R, Kroger M, Eckl C, Gitzelmann S, Vilne B, Bock F, Graf S, Schiemann M, Keller UB, Peschel C, et al. Stromal pleiotrophin regulates repopulation behavior of hematopoietic stem cells. Blood. 2011; 118:2712–2722. [PubMed: 21791434]

Kahn J, Byk T, Jansson-Sjostrand L, Petit I, Shivtiel S, Nagler A, Hardan I, Deutsch V, Gazit Z, Gazit D, et al. Overexpression of CXCR4 on human CD34+ progenitors increases their proliferation, migration, and NOD/SCID repopulation. Blood. 2004; 103:2942–2949. [PubMed: 15070669]

Kiel MJ, Morrison SJ. Uncertainty in the niches that maintain haematopoietic stem cells. Nat Rev Immunol. 2008; 8:290–301. [PubMed: 18323850]

Kiel MJ, Yilmaz OH, Iwashita T, Terhorst C, Morrison SJ. SLAM family receptors distinguish hematopoietic stem and progenitor cells and reveal endothelial niches for stem cells. Cell. 2005; 121:1109–1121. [PubMed: 15989959]

Laughlin MJ, Eapen M, Rubinstein P, Wagner JE, Zhang MJ, Champlin RE, Stevens C, Barker JN, Gale RP, Lazarus HM, et al. Outcomes after transplantation of cord blood or bone marrow from unrelated donors in adults with leukemia. N Engl J Med. 2004; 351:2265–2275. [PubMed: 15564543]

Li YS, Milner PG, Chauhan AK, Watson MA, Hoffman RM, Kodner CM, Milbrandt J, Deuel TF. Cloning and expression of a developmentally regulated protein that induces mitogenic and neurite outgrowth activity. Science. 1990; 250:1690–1694. [PubMed: 2270483]

Lo Celso C, Lin CP, Scadden DT. In vivo imaging of transplanted hematopoietic stem and progenitor cells in mouse calvarium bone marrow. Nat Protoc. 2011; 6:1–14. [PubMed: 21212779]

Malard F, Kroger N, Gabriel IH, Hubel K, Apperley JF, Basak GW, Douglas KW, Geraldes C, Jaksic O, Koristek Z, et al. Plerixafor for autologous peripheral blood stem cell mobilization in patients previously treated with fludarabine or lenalidomide. Biol Blood Marrow Transplant. 2012; 18:314–317. [PubMed: 22001752]

Mendez-Ferrer S, Michurina TV, Ferraro F, Mazloom AR, Macarthur BD, Lira SA, Scadden DT, Ma'ayan A, Enikolopov GN, Frenette PS. Mesenchymal and haematopoietic stem cells form a unique bone marrow niche. Nature. 2010; 466:829–834. [PubMed: 20703299]

Meng K, Rodriguez-Pena A, Dimitrov T, Chen W, Yamin M, Noda M, Deuel TF. Pleiotrophin signals increased tyrosine phosphorylation of beta beta-catenin through inactivation of the intrinsic

catalytic activity of the receptor-type protein tyrosine phosphatase beta/zeta. Proc Natl Acad Sci U S A. 2000; 97:2603–2608. [PubMed: 10706604]

Ochiai K, Muramatsu H, Yamamoto S, Ando H, Muramatsu T. The role of midkine and pleiotrophin in liver regeneration. Liver Int. 2004; 24:484–491. [PubMed: 15482347]

Papayannopoulou T, Craddock C, Nakamoto B, Priestley GV, Wolf NS. The VLA4/VCAM-1 adhesion pathway defines contrasting mechanisms of lodgement of transplanted murine hemopoietic progenitors between bone marrow and spleen. Proceedings of the National Academy of Sciences of the United States of America. 1995; 92:9647–9651. [PubMed: 7568190]

Raulo E, Chernousov MA, Carey DJ, Nolo R, Rauvala H. Isolation of a neuronal cell surface receptor of heparin binding growth-associated molecule (HB-GAM). Identification as N-syndecan (syndecan-3). J Biol Chem. 1994; 269:12999–13004. [PubMed: 8175719]

Rocha V, Labopin M, Sanz G, Arcese W, Schwerdtfeger R, Bosi A, Jacobsen N, Ruutu T, de Lima M, Finke J, et al. Transplants of umbilical-cord blood or bone marrow from unrelated donors in adults with acute leukemia. N Engl J Med. 2004; 351:2276–2285. [PubMed: 15564544]

Salter AB, Meadows SK, Muramoto GG, Himburg H, Doan P, Daher P, Russell L, Chen B, Chao NJ, Chute JP. Endothelial progenitor cell infusion induces hematopoietic stem cell reconstitution in vivo. Blood. 2009; 113:2104–2107. [PubMed: 19141867]

Stoica GE, Kuo A, Aigner A, Sunitha I, Souttou B, Malerczyk C, Caughey DJ, Wen D, Karavanov A, Riegel AT, et al. Identification of anaplastic lymphoma kinase as a receptor for the growth factor pleiotrophin. J Biol Chem. 2001; 276:16772–16779. [PubMed: 11278720]

Sugiyama T, Kohara H, Noda M, Nagasawa T. Maintenance of the hematopoietic stem cell pool by CXCL12-CXCR4 chemokine signaling in bone marrow stromal cell niches. Immunity. 2006; 25:977–988. [PubMed: 17174120]

Tang W, Li Y, Osimiri L, Zhang C. Osteoblast-specific transcription factor Osterix (Osx) is an upstream regulator of Satb2 during bone formation. The Journal of Biological Chemistry. 2011; 286:32995–33002. [PubMed: 21828043]

Tezuka K, Takeshita S, Hakeda Y, Kumegawa M, Kikuno R, Hashimoto-Gotoh T. Isolation of mouse and human cDNA clones encoding a protein expressed specifically in osteoblasts and brain tissues. Biochemical and Biophysical Research Communications. 1990; 173:246–251. [PubMed: 1701634]

Zhang J, Niu C, Ye L, Huang H, He X, Tong WG, Ross J, Haug J, Johnson T, Feng JQ, et al. Identification of the haematopoietic stem cell niche and control of the niche size. Nature. 2003; 425:836–841. [PubMed: 14574412]

Zon LI. Intrinsic and extrinsic control of haematopoietic stem-cell self-renewal. Nature. 2008; 453:306–313. [PubMed: 18480811]

Highlights

- Pleiotrophin regulates hematopoietic stem cell self-renewal in vivo
- Deletion of PTPRZ amplifies the hematopoietic stem cell pool
- Pleiotrophin is expressed and secreted by bone marrow endothelial cells
- Pleiotrophin regulates hematopoietic progenitor cell homing and retention

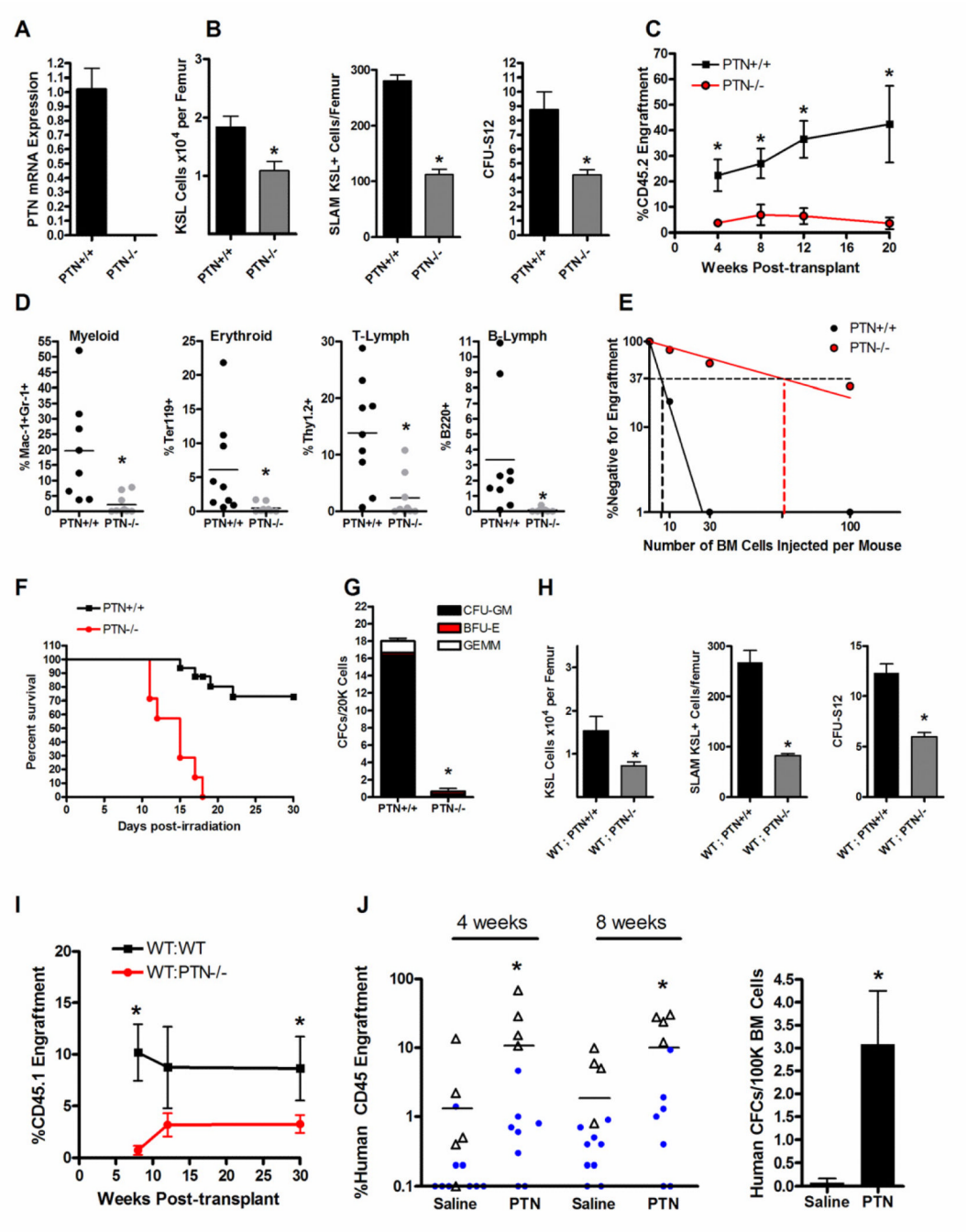

Figure 1. PTN Regulates HSC Self-Renewal and is Necessary for Hematopoietic Regeneration In Vivo

(A) Quantitative RT-PCR of PTN expression in the BM of PTN$^{-/-}$ mice and PTN$^{+/+}$ mice. (B) PTN $^{-/-}$ mice contained significantly decreased BM KSL cells/femur, SLAM^{+}KSL (CD150^{+}CD48^{-}CD41^{-}lin^{-}c-kit^{+}sca-1^{+}) cells/femur, and BM CFU-S12 compared to PTN$^{+/+}$ mice (n=4 for KSL, n=3 for SLAM^{+}KSL, n=5 for CFU-S12; * p = 0.01, * p = 0.0002, * p = 0.003 respectively). (C) CD45.1^{+} mice transplanted competitively with a limiting dose (30 cells) of BM CD34^{-}KSL cells from CD45.2^{+} PTN $^{-/-}$ mice demonstrated significantly decreased donor CD45.2^{+} cell engraftment over time compared to mice transplanted with the identical dose of BM CD34^{-}KSL cells from PTN $^{+/+}$ mice (n=6-10 mice/group; 4 wks, *

p=0.007; 8 wks, * p=0.006; 12 wks, * p=0.0008; 20 wks, * p = 0.02). (D) 12 week myeloid (Mac-1^+), erythroid (Ter119$^+$), T-cell (Thy 1.2^+), and B-cell (B220$^+$) cell engraftment (* p=0.004, * p=0.01, * p=0.002, and * p=0.02, respectively, for differences between recipients of BM from PTN $^{+/+}$ and PTN $^{-/-}$ mice). (E) Poisson statistical analysis after limiting dilution transplant assay. Plots were obtained to allow estimation of CRU frequency in PTN $^{+/+}$ and PTN $^{-/-}$ mice (n=9-10 mice transplanted at each cell dose per condition). The plot shows the percentage of recipient (CD45.1^+) mice containing < 1% CD45.2^+ cells (non-engrafted) in the PB at 12 weeks post-transplantation (Y axis) versus the number of cells injected per mouse (X axis). The horizontal line indicates the point where 37% of the mice are non-engrafted; the vertical lines highlight the CRU frequencies in each mouse (PTN$^{-/-}$ mice, 1/66, versus PTN $^{+/+}$ mice, 1/6). (F) PTN $^{-/-}$ mice displayed increased radiosensitivity compared to PTN $^{+/+}$ mice and failed to regenerate hematopoiesis following total body irradiation (TBI). Sixty-nine percent (11 of 16) of PTN $^{+/+}$ mice were alive at day +30 following 700 cGy TBI (at left). Conversely, none of the PTN $^{-/-}$ mice (0 of 7) survived beyond day +18 ($p<0.0001$, log rank analysis). (G) PTN $^{-/-}$ mice contained > 15-fold decreased BM colony forming cells (CFCs) at day +20 following TBI compared to PTN $^{+/+}$ mice (at right, n=3/group, * p=0.01). (H) WT;PTN $^{-/-}$ mice contained decreased BM KSL cells, decreased SLAM$^+$KSL HSCs, and decreased CFU-S12 compared to WT;PTN$^{+/+}$ mice (means ± SEM, n=8-9 for KSL and CFU-S12; n=3 for SLAM analysis; KSL, * p = 0.02; SLAM$^+$KSL, * p = 0.02; CFU-S12, * p =0.002). (I) Mice competitively transplanted with a limiting dose (30 cells) of BM CD34$^-$KSL cells from WT;PTN $^{-/-}$ mice demonstrated significantly lower donor CD45.1^+ cell engraftment over 4 - 30 weeks compared to mice transplanted with the identical dose of CD34$^-$KSL cells from WT;PTN $^{+/+}$ mice (n=8 mice/group; 8 wks, * p=0.001; 30 wks, * p = 0.04. Error bars represent SEM for all experiments; Student's t test was performed for comparisons). (J) NOD-SCID IL2R$\gamma^{-/-}$ (NSG) mice were irradiated with 250 cGy and then transplanted with human CB mononuclear cells (5-10 × 10^5 cells/mouse; Experiment 1 represented by blue circles; Experiment 2 represented by open triangles) followed by intraperitoneal injections of 2 or 4 g PTN or saline on days +7, +10, and +13 post-transplant. PTN-treated mice displayed significantly increased human hematopoietic cell engraftment in the peripheral blood over time post-transplant compared to saline-treated controls (at left, n = 11-14 per group, 4 weeks *p = 0.04; 8 weeks *p=0.03). Horizontal bars represent mean levels of donor human CD45$^+$ cell engraftment. Transplanted NSG mice that were treated with PTN demonstrated significantly increased human colony forming cells (CFCs) in the BM at 8 weeks compared to saline-treated NSG mice (at right, n = 4 mice/group, * p = 0.02).

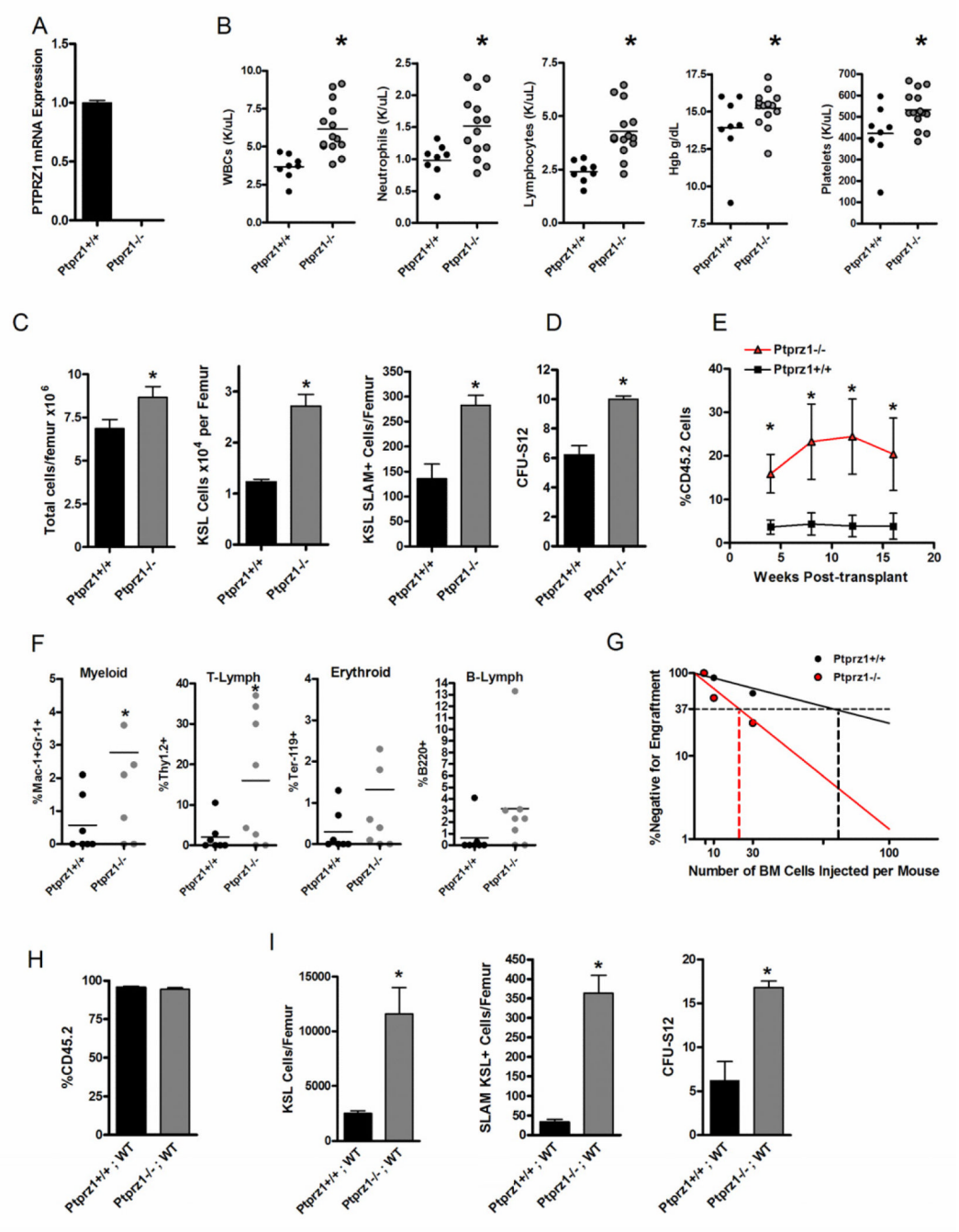

Figure 2. Deletion of PTPRZ is Sufficient to Expand the BM HSC Pool

(A) Quantitative RT-PCR analysis of PTPRZ expression in Ptprz1$^{+/+}$ and Ptprz1$^{-/-}$ mice. (B) Scatter plots show the complete blood counts in the PB of Ptprz1$^{+/+}$ mice compared to Ptprz1 $^{-/-}$ mice (WBCs,* p = 0.005; Neutrophils, * p = 0.006; Lymphocytes, * p= 0.003; Hgb, * p = 0.04; Platelets, * p = 0.01). Mean values are represented by horizontal lines; n=8-13 mice per condition. (C) Ptprz1 $^{-/-}$ mice demonstrate increased mean BM cell counts, KSL cells/femur and SLAM^{+}KSL cells/femur compared to Ptprz1$^{+/+}$ mice (n=3-5 mice/group; * p = 0.04, * p = 0.003, * p = 0.002, respectively). Error bars represent SEM. (D) Ptprz1$^{-/-}$ mice contain increased BM CFU-S12 compared to Ptprz1$^{+/+}$ mice (n = 7-9/group, p < 0.0001). (E) Mice transplanted with a limiting dose (30 cells) of BM CD34^{-}KSL cells

from Ptprz1$^{-/-}$ mice demonstrated significantly higher donor CD45.2^{+} donor cell engraftment over time compared to recipients of the identical dose of CD34^{-}KSL cells from Ptprz1$^{+/+}$ mice (means ± SEM are shown, n = 7-10 mice/group; 4 wks, * p = 0.01; 8 wks, * p = 0.03; 12 wks, * p = 0.03; 16 wks, *p = 0.04. Student's t test for all comparisons). (F) Multilineage engraftment of myeloid, erythroid, T-cells, and B-cells is shown at 12 weeks post-transplantation; n = 7-8 mice/group, Myeloid, * p = 0.03; T-cell, * p = 0.02. (G) Poisson statistical analysis after limiting dilution transplant assay; plots were obtained to allow estimation of CRU frequency in Ptprz1$^{+/+}$ mice (1 in 72) and Ptprz1$^{-/-}$ mice (1 in 23); n = 7-8 mice transplanted at each cell dose per condition. (H) The mean percent donor chimerism is shown at 8 weeks post-transplantation of BM cells from Ptprz1$^{+/+}$ or Ptprz1$^{-/-}$ mice (CD45.2^{+}) into lethally irradiated Bl6.SJL recipient (CD45.1^{+}) mice (WT) to generate chimeric Ptprz1$^{-/-}$;WT mice and Ptprz1$^{+/+}$;WT mice. Mean donor cell chimerism was ≥95% in Ptprz1$^{-/-}$;WT mice and Ptprz1$^{+/+}$;WT mice (n = 4-5 mice/group, means ± SEM). (I) Ptprz1$^{-/-}$;WT mice contained significantly increased BM KSL cells/femur, SLAM^{+}KSL cells/femur and CFU-S12 compared to Ptprz1$^{+/+}$;WT mice (n = 3-6/group, * p = 0.004, * p < 0.0001, and * p = 0.002, respectively). Data represent means ± SEM; Student's t test for comparisons.

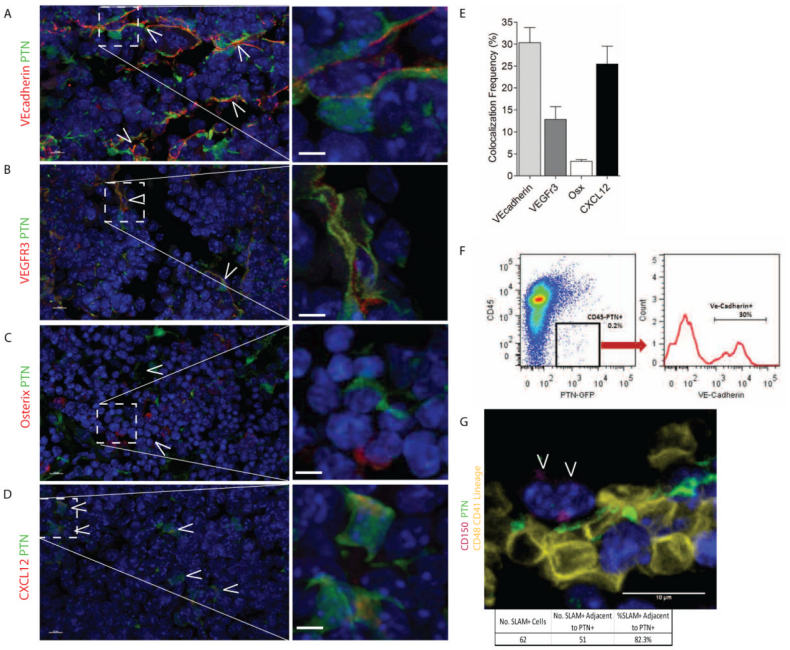

Figure 3. PTN Is Expressed by BM Endothelial Cells in the HSC Niche

(A) PTN-GFP reporter mice stained with VE-cadherin antibody (red) demonstrate that VE-cadherin$^+$ ECs express PTN (green). White arrows indicate cells which express both PTN and VE-cadherin. Inset box is shown magnified at right, white scale bar represents 10 μm. (B) VEGFR3$^+$ sinusoidal vessels (red) are shown which co-express PTN (green). White arrows indicate cells expressing both VEGFR3 and PTN; high power image at right. (C) Staining for osterix$^+$ cells (red) indicates that very few osterix$^+$ cells express PTN (green); high power image at right. (D) CXCL12-abundant reticular cells (CARs, red) were identified which co-expressed PTN (green). White arrows indicate cells expressing both PTN and CXCL12. (E) Quantification of percentage of VE-cadherin$^+$, VEGFR3$^+$, osterix (Osx)$^+$, and CXCL12$^+$ cells which co-expressed PTN. Osterix$^+$ cells had the lowest amount of co-localization with PTN-GFP$^+$ cells (3.3%), while 30% of VE-cadherin cells, 12.8% of VEGFR3$^+$ cells and 25.5% of CXCL12$^+$ cells co-expressed PTN (n=2-6 tissue sections/stain, Bars represent means +/− SEM). (F) Representative FACS analysis of BM cells from PTN-GFP reporter mice co-stained with CD45 and VE-cadherin antibodies, demonstrating that PTN is expressed by VE-cadherin$^+$ cells. (G) Immunohistochemical staining for CD150$^+$CD48$^-$CD41$^-$lineage$^-$ cells in the femurs of PTN-GFP mice was performed. A representative image is shown. 82.3% (51 of 62) of the CD150$^+$CD48$^-$CD41$^-$lineage$^-$ cells (magenta) were within a 5 micron distance of PTN$^+$ (green) cells in the BM (30 images analyzed from 5 femur sections).

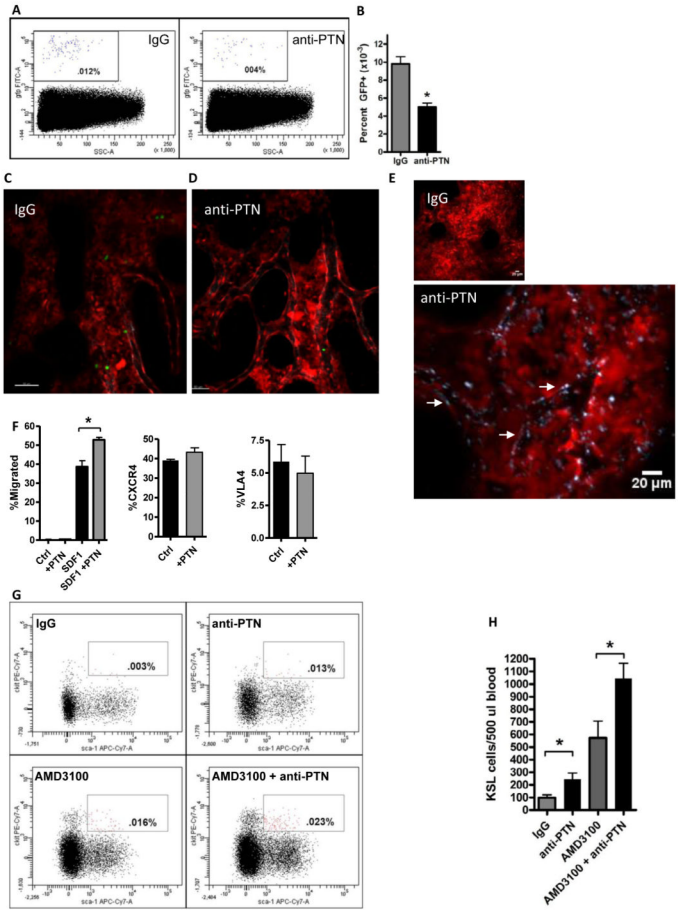

Figure 4. PTN Regulates the Homing and Retention of BM HSPCs

(A) Systemic administration of anti-PTN significantly decreased HSPC homing to the BM niche. Representative FACS analysis is shown of percentage GFP^+ donor hematopoietic cells in the BM of recipient C57Bl6 mice at 18 hours following intravenous infusion of BM Sca-1^+lin$^-$$GFP^+$ cells after pre-treatment of recipient mice with either anti-PTN or IgG. (B) Anti-PTN treated mice contained > 2-fold decreased donor GFP^+ cells in the BM at 18 hours post-infusion compared to IgG-treated control mice. n=5-6/group, means ± SEM, *p=0.0004. (C, D) Administration of anti-PTN inhibits the lodgment and transmigration of HPCs from the BM vasculature into the stem cell niche. Representative intravital images are shown of the calvarial BM space in living dsRed mice during the first 4 hours post-intravenous infusion of 3×10^6 BM lin$^-$$GFP^+$ cells. Mice that were pre-treated with IgG antibody (C) demonstrated abundant homing of transplanted cells (green) from the BM sinusoidal vasculature (gray) into the niche, whereas mice pre-treated with anti-PTN displayed a markedly decreased number of donor HPCs within the extravascular BM space (D). A single GFP^+ (green) cell is shown within the BM vasculature in the anti-PTN treated mice. See also Movies S1 and S2 for dynamic imaging of donor GFP^+ hematopoietic progenitor cell homing in the BM of IgG-treated and anti-PTN treated mice. (E) Systemically administered anti-PTN binds extensively to the BM sinusoidal vasculature. Representative intravital imaging is shown of the calvarial BM of dsRed mice at 30 minutes after intravenous injection of either IgG-DyLight650 antibody (left, 20×, scale bar 50 μm) or anti-PTN-DyLight650 (middle, 20X, scale bar 50 μm). Binding and illumination of the BM sinusoidal vasculature by anti-PTN antibody (gray outline, white arrows) is shown in high power at right (4 times zoom of white box area in previous image, scale bar 20 μm). (F) Pre-

incubation with PTN augments HPC migration to an SDF1 gradient. BM ckit^{+}lin^{-} cells demonstrated no migration to media alone or PTN in a 4 hour transwell assay (left, n=4/group). A percentage of BM ckit^{+}lin^{-} cells migrated to an SDF1 gradient in the lower chamber of transwell cultures. BM ckit^{+}lin^{-} cells that were pre-incubated with PTN × 1 hour demonstrated significantly increased migration to SDF1 compared to control cultures at 4 hours in transwell assay. n=6/group, means ± SEM, *p=0.002 (left). Incubation of BM ckit^{+}lin^{-} cells with PTN had no effect on cell surface expression of CXCR4 (middle) or VLA4 (right); n=6/group, means ± SEM. (G) Administration of anti-PTN promoted the rapid mobilization of HSPCs in wild type mice. Representative FACS plots are shown of the percentage of KSL cells in the PB of adult C57Bl6 mice at 1 hour following intravenous administration of IgG, anti-PTN, AMD3100 or AMD3100 + anti-PTN. Both anti-PTN and AMD3100 increased the mobilization of KSL cells to the PB compared to IgG-treated control mice. Mice treated with AMD3100 + anti-PTN displayed increased KSL cell mobilization compared to AMD3100 treatment alone. (H) The bar graphs show the means ± SEM of KSL cells in the PB of IgG-treated mice, anti-PTN treated mice, AMD3100-treated mice and mice treated with AMD3100 + anti-PTN. Treatment with anti-PTN alone or in combination with AMD3100 significantly increased KSL cell mobilization compared to IgG-treated or AMD3100-treated mice, respectively. *p=0.02 for anti-PTN versus IgG (n=8/group, means ± SEM), *p=0.03 for AMD3100 + anti-PTN versus AMD3100 alone (n=5/group, means ± SEM).

Table 1

Gene Expression of VEcadherin^{+}PTN^{+} Cells

		Fold Difference	
Gene	**Description**	**VEcad$^{\pm}$PTN$^{\pm}$**	**p value**
VEGFR2	Vascular endothelial growth factor receptor 2	84.7	0.006
VEGFR3	Vascular endothelial growth factor receptor 3	68.1	0.02
CXCL12	Chemokine CXC ligand 12	48.0	0.003
LepR	Leptin receptor	136.2	0.02
Nestin	Nestin	ND	

Bone marrow cells were collected from PTN-GFP reporter mice and stained with anti-VEcadherin or isotype antibody. FACS was performed to collect VEcad^{+}PTN^{+} cells and RNA was isolated for qRT-PCR analysis for the genes identified at left. The fold differences in gene expression between VEcad^{+}PTN^{+} cells versus CD45^{+}PTN^{-} BM cells are shown. n=3 replicates/group; t test; ND= not detected.